Effect of Ceria Doping in Different Impregnation Steps on Ni-Based Catalysts Loading on TiO$_2$-SiC for CO Methanation

Chen Liu [1], Qin Zheng [1,*] and Yusheng Zhang [2,*]

1   College of Medicine and Pharmaceutical Engineering, Shijiazhuang Vocational College of Technology and Information, Shijiazhuang 050500, China; liuchen0222@outlook.com
2   Institute for Development of Energy for African Sustainability (IDEAS), University of South Africa (UNISA), Private Bag X6, Florida 0710, South Africa
*   Correspondence: qinzheng2022@outlook.com (Q.Z.); 54137403@mylife.unisa.ac.za (Y.Z.); Tel.: +86-158-9853-9867 (Y.Z.)

Abstract: A series of TiO$_2$-SiC supported Ni-based catalysts with and without ceria doping were prepared by a traditional impregnation method. CeO$_2$ was introduced into the catalyst in different steps of the impregnation process. All the samples were characterized by N$_2$ physisorption, XRD, TPR, and TGA, and were tested for the performance of CO methanation in a fixed-bed reactor under atmospheric conditions through the steam of H$_2$/CO = 3 without diluent gas. All the Ni-based catalysts supported by TiO$_2$-SiC exhibited the property of anti-sintering and could efficiently avoid carbon deposition occurring on catalysts. The experimental results show that the performance of all CeO$_2$ doping samples (more than 80% of CO conversion) was better than the sample without CeO$_2$ (around 20% of CO conversion). Introducing CeO$_2$ after the dry step of impregnation achieved complete CO conversion at a lower temperature compared with its introduction through doping at the co-impregnation and step-impregnation methods. The results of further characterization indicate that the addition of CeO$_2$ in different impregnation steps affected the dispersion of nickel on support, made the size of metal particles smaller, and changed the reducibility of catalysts.

1. Introduction

Since the methanation reaction between carbon oxide and hydrogen was reported for the first time by Sabatier and Senderens in 1902 [1], this reaction has received wide attention as the most important step in the production process of synthetic natural gas (SNG) [2,3]. As mentioned, the research and application of CO methanation reaction has focused on two aspects: removing a small quantity of CO in ammonia plants or proton-exchange membrane fuel cells in which CO poisons an anode catalyst [4,5]; and converting coal or biomass to synthesize substituted natural gas [6–8]. As natural gas is a clean, safe, and convenient transport fossil fuel, its proportion in world energy consumption is growing. The "golden age" of utilizing natural gas in the United States was the period after the Second World War until the 1970s [9]. In recent years, natural gas has become the fastest-growing fossil fuel in the world and its consumption has increased from 2000 bcm in 1990 to over 4000 bcm in 2019 [10]. Due to the increasing gap between consumers' demand and output, the SNG production from other carbon sources becomes more attractive.

The catalyst used in a methanation reaction is normally a supported catalyst, and several metallic elements exhibit catalytic activity, such as Ru [11], Fe [12], Co [13], and Ni [14–16]. Because of its relatively low price, high catalytic activity, and high methane selectivity, Ni-based catalysts are widely used as an industrial catalyst for SNG [14]. It is well known that CO methanation is an extremely exothermic reaction [2]. It could cause temperature increase in catalyst bed and lead to catalyst deactivation, which was reported

by Eisenlohr et al. [17]. As mentioned in other work, in the adiabatic condition for the ratio of $H_2/CO = 3$ at 3 MPa with an inlet temperature of 300 °C, the inner temperature increased to 623 °C with the hot spot in the bed reaching even higher [18]. This high temperature easily leads to the sinter of catalysts, and in some cases carbon deposition can occur because of methane cracking and carbon monoxide disproportionation. One of the methods to solve this problem is employing a support with high thermo-conductivity and thermo-stability. Compared with some common supports used in lab research and industrial plants such as Al_2O_3 [19], SiO_2 [20] and TiO_2 [21], silica carbide (SiC) exhibits more excellent properties i.e., high mechanical strength, high thermal stability, and especially great thermal conductivity, which has attracted more attention in recent years. Yu et al. have reported that Ni-based catalyst loading in SiC can efficiently avoid the sintering of nickel particles [22]. Moreover, Liu et al. [23] have reported that, compared with Ni/Al_2O_3, Ni/SiC is thermally stable and highly resistant to carbon deposition even at 600 °C over 100 hrs. However, because of the weak interaction between SiC and the catalytic metal, the adsorption of nickel on the SiC support becomes a problem. To solve this problem, one approach is to add another element to the SiC formatting composited support. TiO_2, which has the properties of an n-type semiconductor, interacts strongly with metal and can improve the adsorption of catalysts [24]. Using TiO_2 to modify SiC can efficiently increase adsorbing properties of the support. However, catalysts using the composited support, TiO_2-SiC loading Ni, have been little investigated for their CO methanation reaction.

Cerium, a rare earth elementary, has been widely used in the preparation of catalysts as a support or a promoter [23,25–28], because it can improve the activity and stability of catalysts, and can efficiently resist carbon deposition. As reported by Zhou et al. [26], Ni-based catalysts supported by CeO_2 showed an excellent reactivity of CO_2 methanation at 340 °C and atmospheric pressure. Furthermore, Yang et al. have reported that CeO_2-Al_2O_3 was an excellent support for a reverse water–gas shift reaction helping to achieve high degrees of CO_2 conversions [27]. As a promoter, CeO_2 also shows excellent properties in Ni-based catalysts. As mentioned in Santamaria et al.'s work [28], the stability of catalyst Ni/Al_2O_3 for steam reforming of biomass pyrolysis volatiles had been greatly improved by incorporating CeO_2, because it enhanced the gasification of coke precursors. Moreover, Liu et al. have considered the promoter CeO_2 could enhance interaction between Ni and SiC and improved dispersion of Ni active species, which improved catalytic activity and stability for high temperature CO methanation [23]. In Xavier's study [29], they demonstrated that adding 1.5 wt.% CeO_2 into Ni/Al_2O_3 catalyst may improve the reducibility and low-temperature activity of the catalyst, and the main reason for increased catalytic activity was considered to be the electronic interaction between Ni and CeO_2.

In this work, the novel support TiO_2-SiC was used to prepare Ni-based CO methanation catalysts. To clarify the factor of CeO_2 and understand the effect of introducing promotor in different impregnation steps, a comparison among the performance of catalysts with CeO_2 introduced at different impregnation steps, and without CeO_2 doping, was made in a CO methanation reaction.

2. Results

2.1. Catalytic Performance for CO Methanation

2.1.1. Effect of Cerium Doping in Different Impregnation Steps

The performance of CeO_2-doped 10 wt.% Ni/TiO_2-SiC, compared with a non-Ce-doped catalyst, was investigated and shown in Figure 1a. To verify the repeatability and reliability of the experimental results, some experiments, including sample NTS and NCTS(ad), were repeated twice. The results of repeated experiments were very close. Therefore, we consider the response data to be credible and reproducible. From the figure, we can see that the CO conversion of all the samples increased with reaction temperature climbing from 280 °C to 350 °C. This result might be attributed to more active sites of the catalysts after modifying CeO_2 [25,30]. Furthermore, some previous reports have indicated that adding CeO_2 not only relieved the electron-deficient state of surface nickel atoms [31],

but also increased the metal Ni dispersion in the surface of the support [32]. Therefore, the addition of CeO_2 plays a significant factor in improving the activity of Ni-based catalysts in CO methanation reaction. Figure 1a also shows the activity difference among the catalysts doping Ce in different impregnation steps. In reaction temperature at 300 °C, CO conversion of sample 10Ce-Ni/TiO_2-SiC(ad) was 98.44%, while sample NCTS(co) and sample NCTS(st) was 90.56% and 82.89%, respectively. The experimental results show that the introduction of CeO_2 at different stages of impregnation led to significant changes in the reactivity of CO methanation.
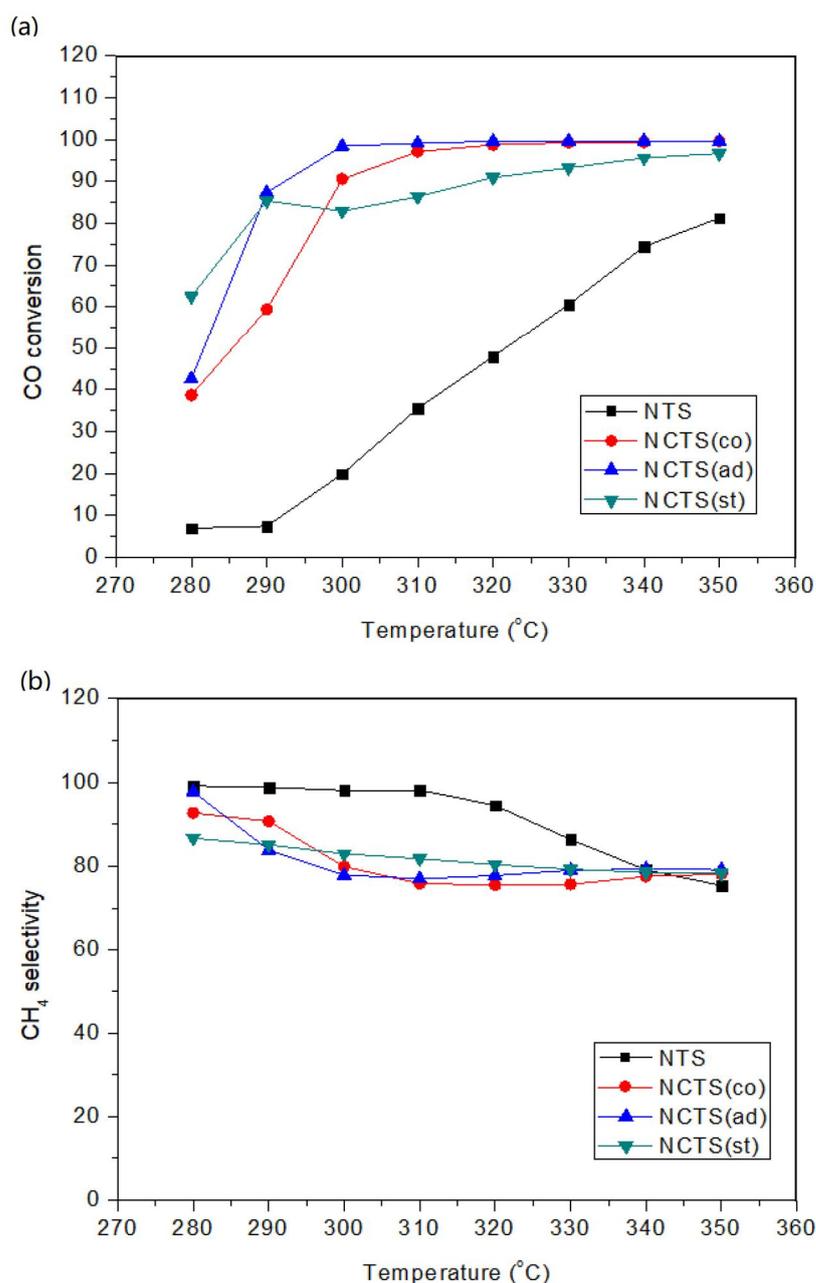
(a)

(b)

Figure 1. Effect of reaction temperature on the (**a**) activities of catalysts (CO conversion) and (**b**) CH_4 selectivity and reaction condition: $H_2/CO = 3$, GHSV = 7500 h^{-1}, atmospheric pressure.

Figure 1b and Table 1 show the CH_4 selectivity and reaction rate of CH_4 generation which was defined as moles of CH_4 generated per gram Ni per second at 300 °C. As shown in Figure 1b, the methane selectivity of all samples was decreased with the rising reaction temperature. Combined with Figure 1a, with CO conversion increasing, the CH_4 selectivity

decreased. This was explained by the fact that the water gas shift synthesis (WGS) occurred. The concentration of H_2O increased with the ongoing methanation reaction, a part of the CO reacted with the H_2O and formed CO_2. This explains the high methane selectivity of the sample NTS below 320 °C. Under those reaction conditions, the CO conversion was less than 50%, and WGS did not take place. A similar result was also confirmed by Hanaa Er-rbib [33]. As shown in Table 1, the sample NCTS(ad) reaction rate of methane generation was 139.3 μmol s^{-1} g^{-1}, which was better than the other three samples. The result proved that introducing CeO_2 after the dry step of impregnation can improve the performance of Ni-based CO methanation catalysts.

Table 1. Rate of CH_4 generation.

Sample	Rate of CH_4 Generation at 300 °C (μmol s^{-1} g^{-1})
NTS	35.5
NCTS(co)	131.6
NCTS(ad)	139.3
NCTS(st)	125.1

2.1.2. Catalyst Stability Test

To investigate the CO methanation long-term stability of samples with doped CeO_2, a group of experiments was conducted at 300 °C, which was the initial stage of CO completely conversion, and kept more than 55 h. The results are shown in Figure 2. From Figure 2, the methanation activity of all the samples was maintained at a high level (CO conversion of more than 95%) in the first 12 h. At this stage, the order of activity of these samples was NCTS(ad) > NCTS(co) > NCTS(st), although the difference was less than 2%. However, with the reaction carried out after 36 h, CO conversion dropped to around 91% of both NCTS(ad) and NCTS(st), while the CO conversion of NCTS(co) decreased to 77%. When the test finished at a TOS of 55 h, the CO conversion of NCTS(ad) and NCTS(st) simultaneously reduced to 82%. At the same condition, the performance of NCTS(co) was worse, only leaving a CO conversion of under 60%, which meant the stability of the sample NCTS(ad) and NCTS(st) was much higher than the sample NCTS(co). The deactivation of the catalyst could be due to the sintering of active metal particles, oxidation of the catalyst, poisoning or carbon deposition on the surface of the catalyst. In addition, the nickel-based catalysts could generate gaseous nickel carbonyl in the presence of CO, which led to the loss of nickel and the decrease of the activity. The reaction gases used in this work were all high-purity cylinder gases, and the possibility of catalyst poisoning was very low. Other deactivation factors need to be inferred from catalyst characterization results.

2.1.3. High Reaction Temperature Stability Test

The high-temperature stability of the sample NCTS (ad) was also studied (Figure 3). As can be seen in Figure 3, CO was almost totally consumed at a reaction temperature ranging from 300 °C to 450 °C, while CO conversion decreased to 93% at 500 °C. On one hand, according to Arrhenius equations, the high temperature helped to increase the initial rate of CO conversion due to the magnitude of the activation energy. On the other hand, it is well known that CO methanation is exothermic so that the low temperature was favorable to reactions occurring thermodynamically. Additionally, F. Haga et al. [34] have reported that the ΔG of the reaction becomes positive when the temperature reaches higher than 530 °C, according to the thermodynamic equilibrium. The higher temperature leads to the occurrence of the steam reforming of methane, which is reversed in methanation. These are in agreement with our experimental results.
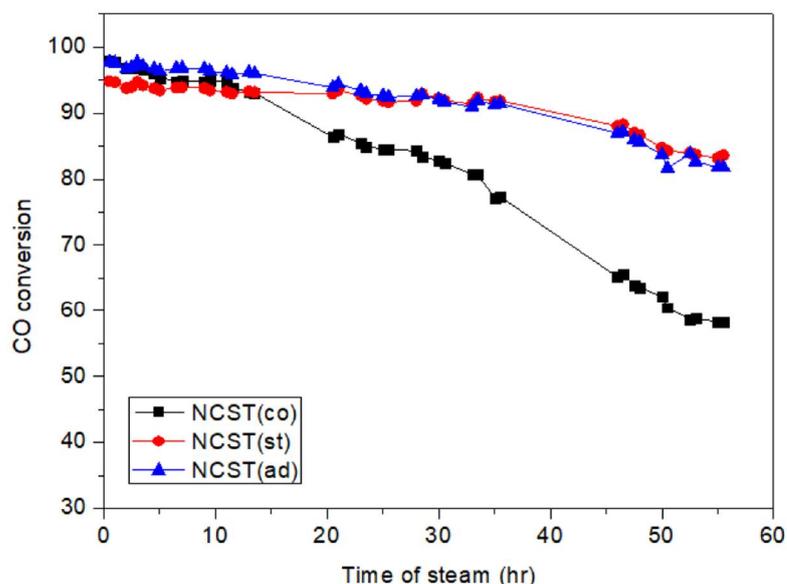
Figure 2. Stability test of result for sample NCTS(co), NCTS(ad) and NCTS(st), reaction condition: $H_2/CO = 3$, T = 300 °C, GHSV = 7500 h^{-1}, atmospheric pressure.
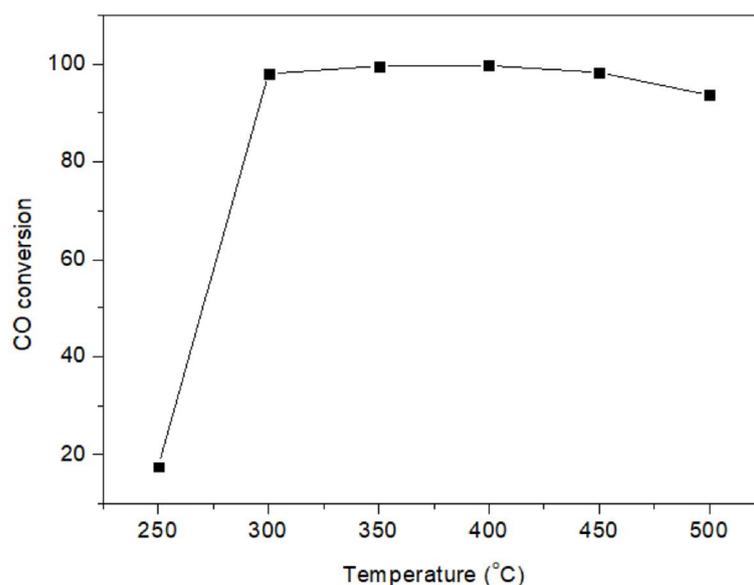

Figure 3. High temperature stability test for sample NCTS(ad), reaction condition: $H_2/CO = 3$, GHSV = 7500 h^{-1}, atmospheric pressure.

2.2. XRD Result

Figure 4 shows the patterns of TiC-SiC and all the samples before and after the methanation reaction. The XRD pattern results of all fresh catalysts are shown in Figure 4a. According to pure face-centered cubic (fcc) NiO phase (JCPDS47-1049), the diffraction peaks at 37.2°, 43.3°, 62.9°, and 75.4° are attributed to NiO planes (111), (200), (220), (311) [35], respectively. For the pattern of TiC-SiC, the reflection peaks at 35.6°, 41.4°, 60°, and 71.8° belong to moissanite-3C SiC (JCPDS29-1129). Meanwhile, the shoulder peaks at 60.5° belong to TiC (JCPDS65-0971), which is consistent with the results of published SICAT [36].
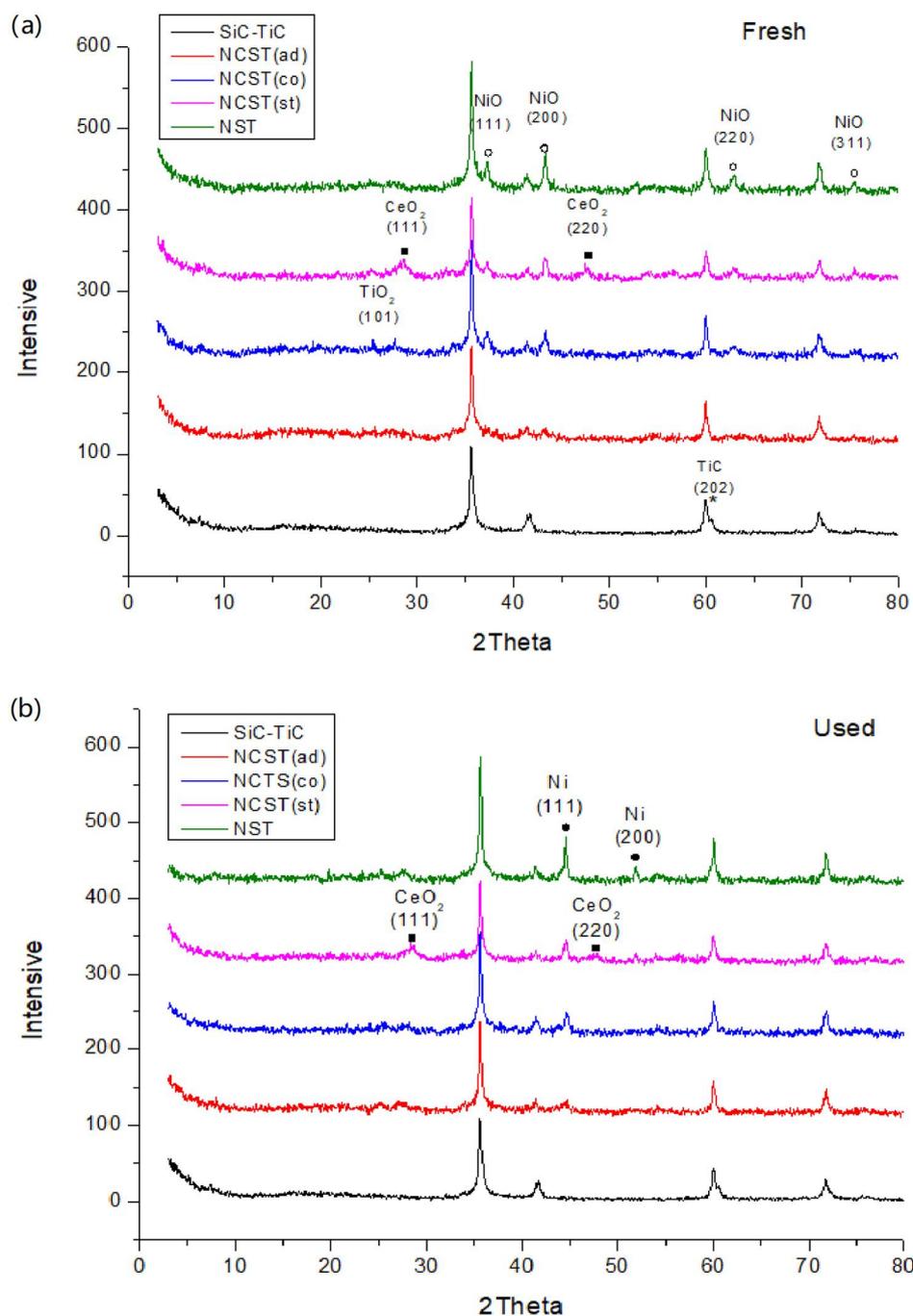
Figure 4. XRD patterns of (**a**) fresh (before reduction) and (**b**) used catalysts.

Figure 4b presents the XRD result of all samples after the methanation. The diffraction peaks at 44.5° and 51.8° are attributed to Ni (JCPDS65-2865) planes (111) and (200) [35]. It can be seen that an insignificant reflection appears at 25.2° in the patterns of all the samples in both Figure 4a,b except for the support TiC-SiC. This peak was indexed to anatase-TiO_2 (JCPDS21-1272) planes (101), which implies TiO_2 generation in the process of calcinations. As mentioned in the report of SICAT [36], when the precursor TiC-SiC underwent an oxidative treatment at 600 °C, the TiC would transfer to both anatase and rutile TiO_2. Moreover, Hu et al. have reported that TiC can be oxidized to TiO_2 at 450 °C for 1 h [37], while the SiC remained unchanged until the calcination temperature reached 1100 °C. As illustrated in Figure 4b, no reflection peaks of carbon can be identified in any XRD pattern of samples, indicating that carbon deposition can be ignored in this experiment.

Interestingly, in both XRD results of the fresh and used sample NCTS(st), two diffraction peaks at 28.5°, and 47.4° appeared, which belong to CeO_2 (JCPDS65-2925), and which is consistent with the results mentioned in the literature [23,27,28]. This result suggests that CeO_2 formed at the preparation process of sample NCTS (st), which is in accordance with our result of the catalysts' activity test in CO methanation (Section 2.1.1). It is worth noting that no characteristic diffraction peaks of NiO were detected in the XRD patterns of all spent catalysts. This result indicates that almost no metallic nickel was oxidized during the reaction.

According to the Scherrer equation [38], the average NiO and nickel crystallite size are calculated by the diffraction peaks of the NiO (200) plane and the Ni (111) plane in Table 2. As shown in the table, all the crystallite sizes of catalysts with CeO_2 doping were smaller than the sample NTS, which indicates that the introduced CeO_2 could effectively reduce the crystallinity of Ni. Moreover, among the catalysts with CeO_2 doping, the sample NCTS(ad) showed the smallest crystallite size. This phenomenon may be caused by the "crystallization-partial dissolution-recrystallization" process of nickel compounds. During the impregnation process, there is a part of water-soluble nickel compound in the catalyst before calcination after drying. It dissolves again during the introduction of CeO_2 and recrystallizes together with CeO_2. Thus, the size of NiO crystals generated after final calcination is reduced. Indeed, this reaction is sensitive to the catalysts' structure property, suggesting that the nickel dispersion degree can have an impact on the activity of catalysts. Smaller nickel crystallite size contributes to higher dispersion degree, thereby obtaining better methanation performance [39]. In addition, from the table, the crystallite size of the fresh and used samples is approximately equal, which indicates that no serious sintering happened in the CO methanation reaction.

Table 2. Crystallite size calculated by the Scherrer equation.

Sample	Fresh NiO Crystallite Size (nm)	Used Ni Crystallite Size (nm)
Ni/TiO_2-SiC	20.4	22.5
$10Ce-Ni/TiO_2$-SiC(co)	17.2	18.1
$10Ce-Ni/TiO_2$-SiC(ad)	14.9	15.3
$10Ce-Ni/TiO_2$-SiC(st)	17.9	18.6

2.3. N_2 Physisorption

Table 3 lists the BET surface of precursor TiC-SiC, support TiO_2-SiC in different impregnation steps, and fresh/used samples of NCTS (ad). After stirring and drying, the surface area of precursor TiC-SiC decreases by 23% of the original value. However, after calcinations in 550 °C for 5 h, the surface area of the support TiO_2-SiC decreased by 58%, compared with TiC-SiC. This result indicates that high-temperature calcinations and mechanical stirring can destroy the physical structure of the support. A similar result has been reported by Zhang et al. [3], who found that severe oxidation could cause more than half of a decrease of the BET surface area of the support SiC. When CeO_2 was introduced into samples at different impregnation steps, the surface areas of supports were different and it would impact the effect of the doped Ce. As shown in the table, the decrease of BET surface area from the support, after calcinations to fresh NCTS(ad), was 19.6%, which might result from the blockage of the pore by impregnated NiO. Compared with the fresh catalyst, the surface area of used NCTS(ad) was kept at the same level, indicating that the support had good thermal resistance after 550 °C calcination.

Table 3. BET results of support, fresh and used 10Ce-Ni/TiO$_2$-SiC(ad).

Sample	S$_{\text{BET}}$ (m^2/g)
TiC-SiC	67.2
TiC-SiC(ad)	51.6
TiO$_2$-SiC	28.1
Fresh NCTS(ad)	22.6
Used NCTS(ad)	22.2

2.4. TG-DSC Analysis of Used Sample NCTS(ad)

The results of the TG-DSC analysis of the reduced and used catalyst sample NCTS(ad) (including after stability test and high-temperature stability test) are shown in Figure 5. From Figure 5a, before 200 °C, a tiny weight loss, less than 1%, can be observed, which can be attributed to the discharging of moisture in the sample. In Figure 5b, the curves of the DSC analysis increased a little bit before 400 °C, which indicates that a portion of the heat was absorbed during the evaporation of the moisture in the sample. In Figure 5a, after 200 °C, a viewable increase of weight can be observed. The increasing weight after all tests might be attributed by the weight changing between metallic Ni and NiO. The oxidation of Ni to NiO is an exothermal reaction, so the overall trend of DSC curves is exothermic. All of these results imply that no carbon deposition on the sample occurred in all the tests. Carbon deposition on the catalyst surface is more likely to occur at high reaction temperatures. The TG-DSC results of the used HT sample show that even under the reaction conditions of 550 °C, no surface carbon formation was detected on the catalyst. This result is in agreement with the previous report [19], which demonstrated that the deactivation of NCTS(ad) catalysts in a methanation reaction did not have any relationship with carbon deposition. In addition, from Figure 5a, we see that the increased weight of the sample after 55 h stability test is less than 1%, which is significantly less than that of the sample after other tests (1.5%). this can be attributed by the loss of nickel. In the presence of CO, metallic nickel could generate gaseous nickel carbonyl under the present reaction conditions, which would cause irreversible nickel loss under the continuous reaction conditions. This phenomenon can be explained by the loss of nickel and matched with our experimental results at stability test (Section 2.1.2).

2.5. H$_2$ Temperature-Programmed Reduction (H$_2$-TPR) Result

To investigate the reduction behavior of nickel oxide in the support TiO$_2$-SiC and to study the influence on this reducibility of introducing CeO$_2$ at different impregnation steps to a catalyst, H$_2$-TPR has been carried out (Figure 6). The overlapping peaks in each TPR result of samples were fitted by three peaks using the Gaussian-type function. The TPR profiles reveal the effect of adding CeO$_2$ at different impregnation steps as a promoter on reduction characteristics of catalysts to some extent. In some literature, due to the different peak temperatures in their TPR profiles, researchers classified the reducible NiO into three types, marked as α-type, β-type, and γ-type [36–38]. Each type of NiO was defined by Zhao et al. [40] as: α-type NiO is surface amorphous NiO or bulk NiO, β-type NiO is the NiO weakly interacting with support, and γ-type NiO is the NiO strongly interacting with support.
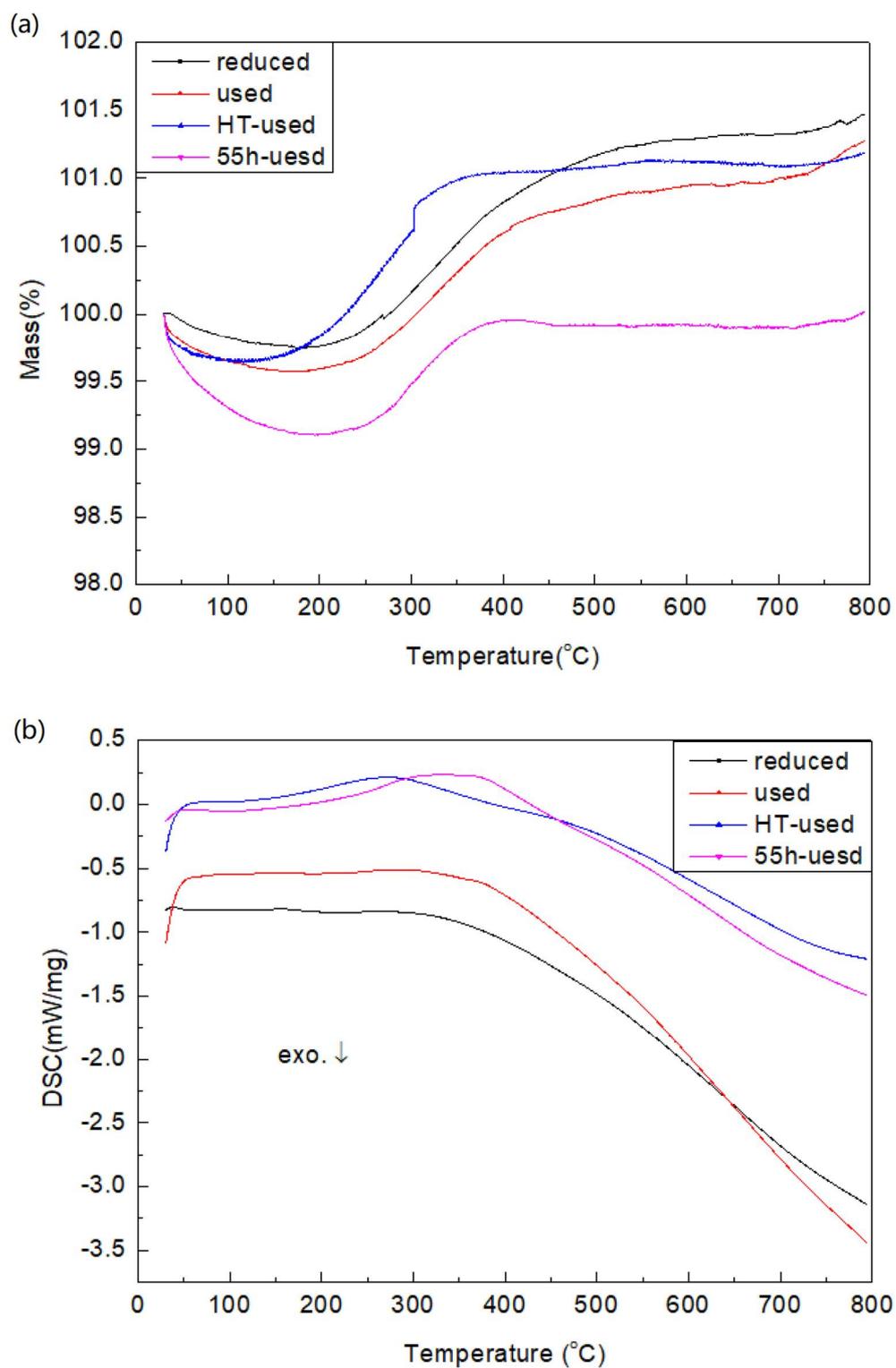
(a)

(b)

Figure 5. TG-DSC profiles of used sample NCTS(ad): (**a**) Thermogravimetric analysis and (**b**) differential scanning calorimetry analysis.
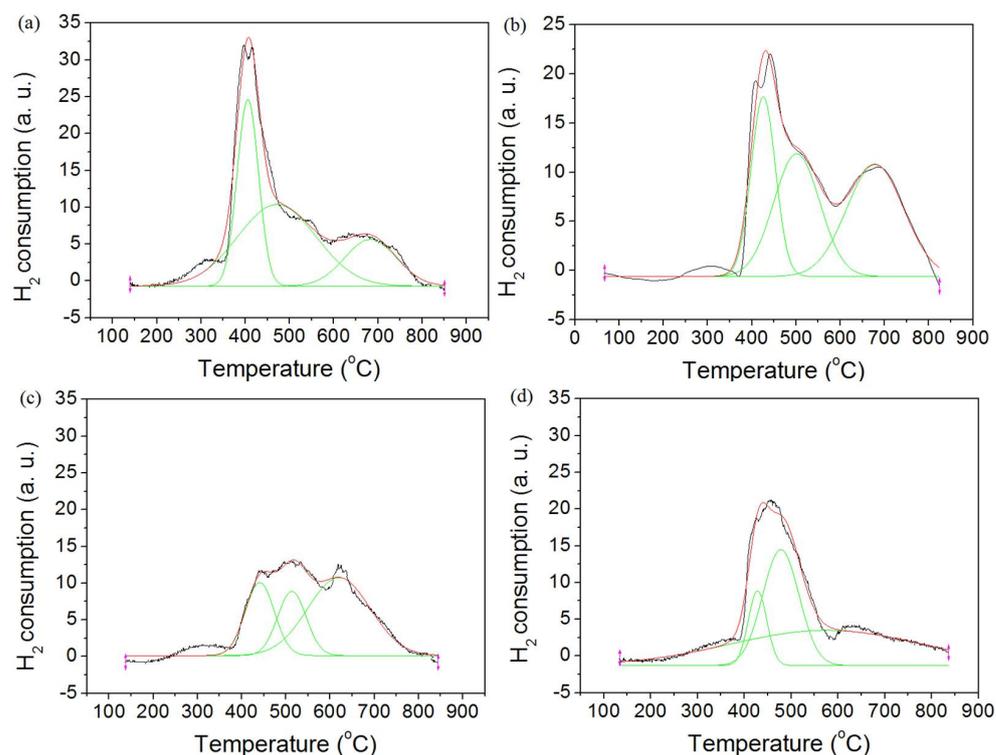
Figure 6. TPR profiles of different catalysts: (**a**) NTS; (**b**) NCTS(co); (**c**) NCTS(ad) and (**d**) NCTS(st).

As observed in Figure 6, the temperature of three elementary peaks in TPR profile of all samples is centered at 400–440 °C, 470–520 °C, and 570–690 °C, respectively. These peaks can be well deconvolved with R^2, which was around 0.98. In addition, each elementary peak in all samples started below 550 °C, which indicates that all the types of NiO could be reduced in our reduction condition. The quantitative results of TPR spectra of the samples with and without doped Ce at different impregnation steps are compared and listed in Table 4. The result demonstrates that, with the CeO_2 introduced, the central temperature of the peaks which represent α-type and β-type shifted upwards. However, for the peak of the γ-type NiO, the central temperature decreased with the addition of CeO_2. A similar phenomenon has been explained by Wang [39], who reports that the partial bonding among the NiO, CeO_2, and support made the electron cloud around NiO asymmetrical and more reactive, consequently improving the reduction degree of NiO species.

Table 4. TPR data of Ni-based catalysts with and without Ce doping in different steps of impregnation.

Sample	Tm (°C)			Fraction of Total Area (%)		
	α	β	γ	α	β	γ
NTS	406	471	683	31.2	50	18.8
NCTS(co)	426	501	678	26.7	34.4	38.9
NCTS(ad)	440	513	619	24	20.8	55.2
NCTS(st)	428	477	574	11.2	34.2	54.6

After mathematical treatment, the proportions of each type of NiO peak area in all catalysts are listed in Table 4. The Ni-based catalyst without Ce doping had the highest fraction of α-NiO and β-NiO, at 31.2% and 50.0%, respectively. At the same time, all the CeO_2 promoted catalysts had higher proportions of γ-NiO, and NCTS(ad) possessed the highest fraction of γ-NiO (55.2%). These results indicate that adding CeO_2 efficiently strengthens the interaction between the NiO and support TiO_2-SiC. Compared with the co-impregnation and step-impregnation methods, introducing CeO_2 into the catalyst after the dry step of the impregnation process exhibited the best effect. As mentioned in some

references [40,41], reducing α-type and β-type NiO easily forms big nickel particles, which exhibit activity at the low reaction temperature. On the contrary, γ-NiO can be reduced to generate the small-size particle, which not only has outstanding activity at low temperatures but also shows a stable activity at high temperature.

3. Materials and Methods

3.1. Catalyst Preparation

The catalysts were prepared by a conventional impregnation method. $Ni(NO_3)_2 \cdot 6H_2O$ was used as metal precursor salts, and TiC-SiC was used as a catalyst support precursor, which would be partially oxidized to become support TiO_2-SiC after the process of calcinations. TiC-SiC is a commercial product provided by SICAT with a specific surface area of 67 m^2/g [36]. To prepare a 10 wt.% Ni/TiO_2-SiC catalyst, 10 g TiC-SiC was added into 100 mL $Ni(NO_3)_2$ aqueous solution, 4.96 g $Ni(NO_3)_2 \cdot 6H_2O$ was dissolved in 100 mL distilled H_2O and stirring for 12 h at room temperature. Then, the slurry was heated at 100 °C until the mixture was dried for 10 h. After these ten hours, the precursors of the catalyst were baked in a muffle furnace heated from room temperature to 600 °C at a rate of 120 °C per hour, and then maintained at 600 °C for 5 h. After calcination, the catalyst was naturally cooled to room temperature for use. Next, cerium oxide was introduced in catalysts by the same impregnation method. $Ce(NO_3)_3 \cdot 6H_2O$ was used as CeO_2 precursor salts. Ce doped at different steps in the process of preparing the catalysts. The amount of doped CeO_2 was 10 wt.% of Ni. No Ce-doped catalysts were indicated as NTS. In the meantime, introducing Ce in Ni-based catalysts at the step of Ni-solution (co-impregnation), after dry, and after calcinations (step-impregnation) are indicated as NCTS(co), NCTS(ad), and NCTS(st), respectively.

3.2. Catalytic Performance

A fixed bed reactor (a 70 cm long stainless tube with an inner diameter of 12 mm) was used to test the performance of the catalysts. The reactor was heated by two PID-regulated ovens, and catalysts were loaded in the flat-temperature zone of the low part of the reactor. In this case, the syngas can be sufficiently preheated by the upper part of the oven without a specialized preheater.

Almost 1.2 mL, or 1.5 g, of the catalysts were placed in the reactor, and all the experiments were performed at atmospheric conditions. Before the catalyst test, the catalyst was reduced at 550 °C and 1 bar on gauge with pure H_2 for 4 h and then decreased to the reaction temperature (280 °C). Reaction gases, which consisted of H_2 and CO (molar ratio of $H_2/CO = 3$, without diluent gas), were supplied from a hydrogen generator and high-pressure gas cylinder, respectively. The flow rate was controlled by mass flow controller (MFC) to ensure a space velocity (GHSV) of 7500 h^{-1}. All the CO methanation tests were conducted at atmospheric pressure. Using Ar as the carrier gas, the feed syngas and tail gas were analyzed by gas chromatograph (SP-6800A6, Tengzhou, China) with TDX-01 column and thermal conductivity detector. All the experimental results of the activity test and high temperature stability test were the average value of three steady-state results obtained after at least four hours of running. The CO conversion (X_{CO}) and CH_4 selectivity (S_{CH4}) were estimated by the following equations:

$$X_{CO}(\%) = (F_{CO,in} - F_{CO,out})/F_{CO,in} \times 100\% \tag{1}$$

$$S_{CH4}(\%) = F_{CH4,out}/(F_{CO,in} - F_{CO,out}) \times 100\% \tag{2}$$

3.3. Catalyst Characterization

X-ray diffraction (XRD) analysis was performed on a Rigaku D/max-2500 diffractometer (Tokyo, Japan), with Cu Kα radiation at 40 kV and 100 mA in a scanning range of 3–80° (2θ). The diffraction peaks of the crystalline phase were compared with those of standard

compounds reported in the JCPDS Date File. Average crystallite sizes of the samples were evaluated from X-ray line broadening analysis (XLBA) by the Scherrer equation:

$$D = K\gamma/B\cos\theta \tag{3}$$

The reducibility of all the catalysts was measured by hydrogen temperature-programmed reduction (H_2-TPR) (Quantachrome, Boynton Beach, FL, USA). The experiments were performed under the mixture of 5% H_2 in N_2 flowing (30 mL/min) over 50 mg of catalysts at a heating rate of 10 °C/min. The uptake amount during the reduction was measured by using a thermal conductivity detector (TCD).

Nitrogen adsorption–desorption isotherms were measured on a Quantachrome Autosorb-1MP sorption analyzer (Boynton Beach, FL, USA) at −196 °C. Before measurement, the samples were degassed at 200 °C for at least 6 h. The specific surface area (SBET) was calculated according to the Brunauer–Emmett–Teller (BET) method ($P/P_0 < 0.1$)

Thermogravimetric analysis (TGA) curves were recorded on a TA SDT Q600 analyzer (New Castle, DE, USA) under a constant airflow of 100 mL/min within a temperature range from room temperature to 850 °C at a heating rate of 10 °C/min in airflow.

4. Conclusions

Ni supported on TiO_2-SiC with and without CeO_2 added at different impregnation steps were prepared by the conventional impregnation method, and their performance of CO methanation and properties were investigated. Ce-doped samples exhibited more activity on methanation reactions than the samples without introduced cerium. From the results of characterizations, the catalysts supported on the support TiO_2-SiC presented the qualities of avoiding sinter and carbon deposition, which could be attributed to the high heat conductivity of the support. Furthermore, adding CeO_2 as a promoter efficiently increases the nickel dispersion degree and smaller particle size, which effectively increases the activity of catalyst on CO methanation. Moreover, the performance of the sample, which introduced CeO_2 after a dry step, was better than that of the other two samples obtained by the co-impregnation method and step-impregnation method. In the process of catalysts preparation, the timing of the introduction of promoter was often overlooked, but it also had a certain impact on the performance of catalysts. This could provide some new ideas for the design and preparation of catalysts.

References

1. Sabatier, P.; Senderens, J.B. New synthesis of methane. *Acad. Sci.* **1902**, *134*, 514–516.
2. Zeng, S.; Gu, J.; Yang, S.; Zhou, H.; Qian, Y. Comparison of techno-economic performance and environmental impacts between shale gas and coal-based synthetic natural gas (SNG) in China. *J. Clean. Prod.* **2019**, *215*, 544–556. [CrossRef]
3. Zhang, G.; Peng, J.; Sun, T.; Wang, S. Effects of the oxidation extent of the SiC surface on the performance of Ni/SiC methanation catalysts. *Chin. J. Catal.* **2013**, *34*, 1745–1755. [CrossRef]
4. Kustov, A.L.; Frey, A.M.; Larsen, K.E.; Johannessen, T.; Nørskov, J.K.; Christensen, C.H. CO methanation over supported bimetallic Ni–Fe catalysts: From computational studies towards catalyst optimization. *Appl. Catal. A Gen.* **2007**, *320*, 98–104. [CrossRef]
5. Zyryanova, M.M.; Snytnikov, P.V.; Gulyaev, R.V.; Amosov, Y.I.; Boronin, A.I.; Sobyanin, V.A. Performance of Ni/CeO_2 catalysts for selective CO methanation in hydrogen-rich gas. *Chem. Eng. J.* **2014**, *238*, 189–197. [CrossRef]
6. Bolt, A.; Dincer, I.; Agelin-Chaab, M. A critical review of synthetic natural gas production techniques and technologies. *J. Nat. Gas. Sci. Eng.* **2020**, *84*, 103670. [CrossRef]

7. Liu, Z.; Chu, B.; Zhai, X.; Jin, Y.; Cheng, Y. Total methanation of syngas to synthetic natural gas over Ni catalyst in a micro-channel reactor. *Fuel* **2012**, *95*, 599–605. [CrossRef]
8. Kopyscinski, J.; Schildhauer, T.J.; Biollaz, S.M.A. Production of synthetic natural gas (SNG) from coal and dry biomass–A technology review from 1950 to 2009. *Fuel* **2010**, *89*, 1763–1783. [CrossRef]
9. Victor, D.G.; Jaffe, A.M.; Hayes, M.H. (Eds.) *Natural Gas and Geopolitics: From 1970 to 2040*; Cambridge University Press: Cambridge, UK, 2006.
10. Liu, J.; Wang, S.; Wei, N.; Chen, X.; Xie, H.; Wang, J. Natural gas consumption forecasting: A discussion on forecasting history and future challenges. *J. Nat. Gas. Sci. Eng.* **2021**, *90*, 103930. [CrossRef]
11. Galletti, C.; Specchia, S.; Specchia, V. CO selective methanation in H_2-rich gas for fuel cell application: Microchannel reactor performance with Ru-based catalysts. *Chem. Eng. J.* **2011**, *167*, 616–621. [CrossRef]
12. Lo, J.M.H.; Ziegler, T. Chemisorption and Reactivity of CHx (x = 0−4) on Fe−Co Alloy Surfaces. *J. Phys. Chem. C* **2008**, *112*, 13642–13649. [CrossRef]
13. Zhou, G.; Wu, T.; Xie, H.; Zheng, X. Effects of structure on the carbon dioxide methanation performance of Co-based catalysts. *Int. J. Hydrogen Energy* **2013**, *38*, 10012–10018. [CrossRef]
14. Zhang, H.; Yunyun, D.; Weiping, F.; Yixin, L.I.A.N. Effects of composite oxide supports on catalytic performance of Ni-based catalysts for CO methanation. *Chin. J. Catal.* **2013**, *34*, 330–335. [CrossRef]
15. Wang, Y.; Wu, R.; Zhao, Y. Effect of ZrO_2 promoter on structure and catalytic activity of the Ni/SiO_2 catalyst for CO methanation in hydrogen-rich gases. *Catal. Today* **2010**, *158*, 470–474. [CrossRef]
16. Li, J.; Li, P.; Li, J.; Tian, Z.; Yu, F. Highly-dispersed Ni-NiO nanoparticles anchored on an SiO_2 support for an enhanced CO methanation performance. *Catalysts* **2019**, *9*, 506. [CrossRef]
17. Eisenlohr, K.H.; Moeller, F.W.; Dry, M. Influence of certain reaction parameters on methanation of coal gas to SNG. [4 refs]. *Am. Chem. Soc. Div. Fuel Chem. Prepr.* **1974**, *19*. Available online: https://www.osti.gov/biblio/7258360 (accessed on 20 February 2022).
18. Rostrup-Nielsen, J.R.; Pedersen, K.; Sehested, J. High temperature methanation: Sintering and structure sensitivity. *Appl. Catal. A Gen.* **2007**, *330*, 134–138. [CrossRef]
19. Galletti, C.; Specchia, S.; Saracco, G.; Specchia, V. CO-selective methanation over Ru–γAl$_2$O$_3$ catalysts in H_2-rich gas for PEM FC applications. *Chem. Eng. Sci.* **2010**, *65*, 590–596. [CrossRef]
20. Shi, P.; Liu, C.J. Characterization of silica supported nickel catalyst for methanation with improved activity by room temperature plasma treatment. *Catal. Lett.* **2009**, *133*, 112–118. [CrossRef]
21. Kamble, V.S.; Londhe, V.P.; Gupta, N.M.; Thampi, K.R.; Grätzel, M. Studies on the Sulfur Poisoning of Ru–RuO_x/TiO_2 Catalyst for the Adsorption and Methanation of Carbon Monoxide. *J. Catal.* **1996**, *158*, 427–438. [CrossRef]
22. Yu, Y.; Jin, G.Q.; Wang, Y.Y.; Guo, X.Y. Synthetic natural gas from CO hydrogenation over silicon carbide supported nickel catalysts. *Fuel Process Technol.* **2011**, *92*, 2293–2298. [CrossRef]
23. Liu, S.S.; Jin, Y.Y.; Han, Y.; Zhao, J.; Ren, J. Highly stable and coking resistant Ce promoted Ni/SiC catalyst towards high temperature CO methanation. *Fuel Process. Technol.* **2018**, *177*, 266–274. [CrossRef]
24. Solymosi, F.; Erdöhelyi, A.; Bansagi, T. Methanation of CO_2 on supported rhodium catalyst. *J. Catal.* **1981**, *68*, 371–382. [CrossRef]
25. Hu, D.C.; Gao, J.J.; Jia, C.M.; Ping, Y.; Jia, L.H.; Wang, Y.L.; XU, G.W.; GU, F.N.; SU, F.B. Research Advances in Methanation Catalysts and Their Catalytic Mechanisms. *Chin. J. Process Eng.* **2011**, *5*, 030.
26. Zhou, G.; Liu, H.; Cui, K.; Jia, A.; Hu, G.; Jiao, Z.; Zhang, X. Role of surface Ni and Ce species of Ni/CeO_2 catalyst in CO_2 methanation. *Appl. Surf. Sci.* **2016**, *383*, 248–252. [CrossRef]
27. Yang, L.; Pastor-Pérez, L.; Gu, S.; Sepúlveda-Escribano, A.; Reina, T.R. Highly efficient Ni/CeO$_2$-Al$_2$O$_3$ catalysts for CO_2 upgrading via reverse water-gas shift: Effect of selected transition metal promoters. *Appl. Catal. B Environ.* **2018**, *232*, 464–471. [CrossRef]
28. Santamaria, L.; Artetxe, M.; Lopez, G.; Cortazar, M.; Amutio, M.; Bilbao, J.; Olazar, M. Effect of CeO_2 and MgO promoters on the performance of a Ni/Al$_2$O$_3$ catalyst in the steam reforming of biomass pyrolysis volatiles. *Fuel Process. Technol.* **2020**, *198*, 106223. [CrossRef]
29. Xavier, K.O.; Sreekala, R.; Rashid, K.K.A.; Yusuff, K.K.M.; Sen, B. Doping effects of cerium oxide on Ni/Al$_2$O$_3$ catalysts for methanation. *Catal. Today* **1999**, *49*, 17–21. [CrossRef]
30. Perkas, N.; Amirian, G.; Zhong, Z.; Teo, J.; Gofer, Y.; Gedanken, A. Methanation of carbon dioxide on Ni catalysts on mesoporous ZrO_2 doped with rare earth oxides. *Catal. lett.* **2009**, *130*, 455–462. [CrossRef]
31. Niu, X.; Yao, Y.; Hao, M.; Wang, X.; Shi, Y.; Xin, M. The role of promoters in the Ni catalyst for methanation (I) the electronic effect caused by the rare earth (La, Ce, Pr and Nd) oxides additives. *J. Mol. Catal.* **1990**, *4*, 9.
32. Maorong, N.; Min, W. Role of Promoters in Ni Catalyst for Methanation (II) Structural and Electronic Effects Caused by Heavy Rare Earth (Dy, Sm, Y, Eu, Yb, Tm, Gd, Er, Tb) Oxide Additives. *J. Mol. Catal.* **1999**, *1*, 21–26.
33. Er-Rbib, H.; Bouallou, C. Methanation catalytic reactor. *C. R. Chim.* **2014**, *17*, 701–706. [CrossRef]
34. Haga, F.; Nakajima, T.; Miya, H.; Mishima, S. Catalytic properties of supported cobalt catalysts for steam reforming of ethanol. *Catal. Lett.* **1997**, *48*, 223–227. [CrossRef]
35. Sun, W.Z.; Jin, G.Q.; Guo, X.Y. Partial oxidation of methane to syngas over Ni/SiC catalysts. *Catal. Commun.* **2005**, *6*, 135–139. [CrossRef]

36. Nguyen, P.; Pham, C. Innovative porous SiC-based materials: From nanoscopic understandings to tunable carriers serving catalytic needs. *Appl. Catal. A Gen.* **2011**, *391*, 443–454. [CrossRef]

37. Hu, J.; Liu, X.; Ding, C. Study on SiC-TiC composite fine powder mixed by vacuum original position and its oxidation susceptibility. *China Ceram.* **2012**, *6*, 009.

38. Ni, Y.; Wang, F.; Liu, H.; Liang, Y.; Yin, G.; Hong, J.; Ma, X.; Xu, Z. Fabrication and characterization of hollow cuprous sulfide ($Cu_{2-x}S$) microspheres by a simple template-free route. *Inorg. Chem. Commun.* **2003**, *6*, 1406–1408. [CrossRef]

39. Wang, Y.Z.; Li, F.M.; Cheng, H.M.; Fan, L.Y.; Zhao, Y.X. A comparative study on the catalytic properties of high Ni-loading Ni/SiO_2 and low Ni-loading $Ni-Ce/SiO_2$ for CO methanation. *J. Fuel Chem. Tech.* **2013**, *41*, 972–977. [CrossRef]

40. Zhao, A.; Ying, W.; Zhang, H.; Hongfang, M.; Fang, D. Ni/Al_2O_3 catalysts for syngas methanation: Effect of Mn promoter. *J. Nat. Gas. Chem.* **2012**, *21*, 170–177. [CrossRef]

41. Zhang, J.; Xu, H.; Jin, X.; Ge, Q.; Li, W. Characterizations and activities of the nano-sized Ni/Al_2O_3 and $Ni/La–Al_2O_3$ catalysts for NH_3 decomposition. *Appl. Catal. A Gen.* **2005**, *290*, 87–96. [CrossRef]